frontiers in Energy Research

ORIGINAL RESEARCH
published: 20 November 2019
doi: 10.3389/fenrg.2019.00132

Microbial Community Rearrangements in Power-to-Biomethane Reactors Employing Mesophilic Biogas Digestate

*Norbert Ács[1], Márk Szuhaj[1], Roland Wirth[1], Zoltán Bagi[1], Gergely Maróti[2], Gábor Rákhely[1,3] and Kornél L. Kovács[1,4]**

[1] Department of Biotechnology, University of Szeged, Szeged, Hungary, [2] Biological Research Centre, Institute of Plant Biology, Szeged, Hungary, [3] Biological Research Centre, Institute of Biophysics, Szeged, Hungary, [4] Department of Oral Biology and Experimental Dental Research, University of Szeged, Szeged, Hungary

OPEN ACCESS

Edited by:
Claire Dumas, Institut National de la Recherche Agronomique (INRA), France

Reviewed by:
Mohanakrishna Gunda, Qatar University, Qatar
Qaisar Mahmood, COMSATS University, Islamabad Campus, Pakistan
Laura Treu, University of Padova, Italy
Stefano Campanaro, University of Padova, Italy

***Correspondence:**
Kornél L. Kovács
kovacs.kornel@bio.u-szeged.hu

Specialty section:
This article was submitted to Bioenergy and Biofuels, a section of the journal Frontiers in Energy Research

Received: *22 January 2019*
Accepted: *04 November 2019*
Published: *20 November 2019*

Citation:
Ács N, Szuhaj M, Wirth R, Bagi Z, Maróti G, Rákhely G and Kovács KL (2019) Microbial Community Rearrangements in Power-to-Biomethane Reactors Employing Mesophilic Biogas Digestate. Front. Energy Res. 7:132. doi: 10.3389/fenrg.2019.00132

The biological conversion of hydrogen (H_2) and carbon dioxide (CO_2) to methane (CH_4), is accomplished by the hydrogenotrophic methanogens (HM). HMs are difficult to cultivate in pure culture, but they are readily available in the mixed culture of effluents from the anaerobic degradation of organic matter, i.e., the fermentation effluent of biogas plants. The rate-limiting step in the work of CH_4-forming microbial communities is the low solubility of H_2 in the aqueous environment. In our approach, the simple fed-batch fermentation technique was selected to supply the gaseous substrates for the microbial community at laboratory scale and mesophilic temperature. Periodically withdrawn samples were analyzed for process parameters and the microbial communities were studied using Terminal Restriction Fragment Length Polymorphism (T-RFLP) of the *mcrA* gene and Ion Torrent whole metagenome DNA sequencing. The metagenome data were evaluated by both read-based and genome-centric bioinformatics tools. The rearrangements in the mixed microbial communities, triggered by switching the operating conditions to biological power-to-biomethane (bio-P2M), have been established. The production rates were 6.30 mL CH_4 L^{-1} h^{-1} during the acclimation phase and 9.21 mL CH_4 L^{-1} h^{-1} by the fully adapted community, respectively. The diversity of the anaerobic microbiota decreased as the bio-P2M process progressed. Feeding the community with H_2 apparently promoted the abundance of several genera, in particular *Candidatus Cloacimonas* and *Herbinix*. The diversity of the *Archaea* community decreased considerably upon daily feeding with H_2 and CO_2. The predominant *Archea* genus was *Methanobacterium* in every reactor, *Methanothrix* persisted for the first 4 weeks, while the initially less abundant genus *Methanoculleus* gained advantage during the adaptation to the sustained bio-P2M process. The accumulation of acetate indicated a strong involvement of homoacetogenic bacteria.

Keywords: biological-power-to-methane, mcrA, T-RFLP, whole genome DNA sequencing, hydrogen, carbon dioxide, acetate

INTRODUCTION

There is a common understanding worldwide about the importance of renewable energy carriers (RECs) and the need for increasing their proportion in the portfolio of the global energy consumption. The rapidly spreading REC technologies comprise primarily wind, photovoltaic, biomass incineration, and hydropower; these approaches generate renewable electricity to be distributed by the power grid. Due to the inherently fluctuating nature of the most widely used wind and photovoltaic technologies, the stable operation of the grid is jeopardized as the fluctuations cannot be synchronized with electricity consumption. Eventually, this leads to the reduction of the overall efficiency and economic feasibility. Among the technical possibilities to overcome this drawback the so-called Power-to-Gas (P2G) concept has gained acceptance (Mazza et al., 2018). The scheme is based on using the excess renewable electricity for water electrolysis to produce oxygen (O_2) and hydrogen (H_2). H_2 is the cleanest energy carrier, however, its widespread direct utilization is severely limited by the underdeveloped technological infrastructure in storage and transportation. Methane (CH_4) is an obvious alternative, as it can equally be exploited as natural gas. The H_2 from water electrolysis is used for biological or chemical conversion of CO_2 to CH_4, the process employing microbes for the CH_4 conversion is called bio-power-to-methane (Angelidaki et al., 2018; Treu et al., 2018a; Nap et al., 2019) The CO_2 to be reduced with H_2 may originate from biogas, which contains 30–50% CO_2 or exhaust gas of internal combustion engines. Through coupling the excess REC electricity utilization with CO_2 mitigation the economic and environmental value of bio-P2M improves (Lewandowska-Bernat, 2017).

The final steps of biogas formation in anaerobic digestion (AD) of organic matter is catalyzed by members of methanogenic archaea. Methanogens have been classified as methylotrophic, acetoclastic and hydrogenotrophic. Methylotrophic methanogens are known to use methyl compounds, such as methanol, dimethyl sulfide, trihalomethanes, chloromethanes, etc. Acetoclastic methanogens produce methane from acetate that is a major intermediate produced from anaerobic digestion of organic matter. Hydrogenotrophic methanogens use CO_2 as an electron acceptor and H_2 as an electron donor. Hydrogenotrophic methanogens can produce bio-methane from a $H_2 + CO_2$ (4:1 molar ratio) (Kougias et al., 2017a). Our previous results suggested that moderate *in situ* increase of the H_2 supply in the reactors by bioaugmentation resulted in elevated CH_4 yields (Bagi et al., 2007; Kovács et al., 2013; Nzila, 2017).

The suitability of the biogas reactor effluent, i.e., the digestate, to carry out the bio-P2M conversion has been demonstrated. With the help of microbes inhabiting the biogas producing community, the process can be effectively carried out (Bassani et al., 2015; Szuhaj et al., 2016; Treu et al., 2018a). The AD digestate microbial community offers the possibility of using a catalyst that is practically free of charge and can be replenished continuously. The exploitation of these benefits and maintaining a stable operation of the community in the bio-P2M reactor, however, requires a thorough knowledge of the members of the complex microbial community and their role in the process in order to avoid malfunctions.

In this paper we therefore examine the microbial background of the biological bio-P2M process by following the rearrangements in the composition of a biogas producing microbial community originated from an industrial biogas plant. This knowledge may lead to the design of reproducible and sustainable microbial systems and extensive management of the bio-P2M technology.

MATERIALS AND METHODS

Fermentation Conditions

Batch fermentations were carried out in serum bottle reactors with 160 mL working volume in triplicates. Each reactor contained 40 mL inoculum from the effluent of an industrial mesophilic biogas plant (Zöldforrás Ltd., Szeged). The biogas facility operates with a substrate mix of pig manure and plant silage (maize and sweet sorghum) in a ratio of 20:80 based on their total organic solid content. The fresh inoculum was filtered upon arrival to exclude solid particles (>0.2 mm) and was kept at 37°C for 10 days to diminish its residual biogas potential. Substrate (0.3 g, α-cellulose: C8002, Sigma) was added to reactors SH and SN (**Table 1**) in a single dose at the start of the experiment. Aluminum crimps and butyl septa were used for airtight sealing and the headspace was flushed with pure nitrogen gas to establish anaerobic condition. The headspace of the reactors CH, SH, and CHw12 received 0.81 ± 0.16 mmol H_2 every day. 0.20 ± 0.11 mmol CO_2 was also dosed to sample CHw12 after signs of CO_2 depletion, i.e., day 27–28 (Szuhaj et al., 2016). Controls (CN, SN, CNw12) received an equal volume of N_2 daily. **Table 1** indicates the gas and substrate composition of the reactors used in this study and the composition of the samples used for T-RFLP and metagenome sequencing, i.e., the inoculum, the samples supplied with H_2 only (CH) or H_2 and substrate (SH) and their corresponding controls, which received N_2 in their head space during the daily gas replacement (CN and SN). The samples for metagenome sequencing were withdrawn on day 28 of the experiment, based upon the fermenters undisturbed behavior at that point, the long term experiments (CNw12 and CHw12) were sampled on day 84. The reactors were incubated in a rotary shaker at 37°C and 160 rpm. The evolved CH_4 and consumed H_2 was determined by gas chromatography (GC) every day. The measured values were normalized employing the ideal gas law at normal temperature of 273 K and normal atmospheric pressure of 1,013 mbar. After the GC measurement, the gas phase was replaced with N_2, using a manifold, and the pressure was adjusted to atmospheric level. This was followed by the injection of the pure H_2 (+ CO_2 in case of CHw12) gas to the selected reactors using sterile disposable syringes and needles. This created an overpressure of about 1.23 bar, which gradually diminished as the gases were converted to CH_4.

Gas Composition Analysis

The gas composition of the headspace was analyzed by an Agilent 6890N GC (Agilent Technologies) equipped with an HP Molsieve 5 Å (30 m × 0.53 mm × 25 μm) column and a TCD detector. The

TABLE 1 | Compositions of the reactors (yellow cells) and samples taken for T-RFLP and metagenome sequencing (green cells).

Sample name	α-Cellulose substrate (0.3 g, single dose)	H_2 addition (daily)	CO_2 addition (daily)	N_2 addition (daily)	Duration (weeks)
Inoculum					0
CH					4
SH					4
CN					4
SN					4
CHw12					12
CNw12					12

injector temperature was 150°C, the measurement was made in splitless mode. The column was maintained at 60°C, the carrier gas was argon HQ 5.0 (Linde) with a flow rate of 16.8 mL min^{-1}. Three biological replicates were used for the measurements.

HPLC Analysis

Weekly withdrawn samples from the liquid phase of the reactors were used to determine the concentrations of volatile fatty acids. Briefly, the samples were centrifuged at 13,000 rpm for 10 min, and the supernatant was filtered using a PES ultracentrifuge filter at 14,000 rpm for 20 min. The supernatant sample was injected into an HPLC (Hitachi LaChrome Elite) equipped with refractive index detector (L-2490). The separation was performed on an ICSep ICE-COREGEL-64H column. The temperature of the column and detector were 50 and 41°C, respectively. The eluent was 0.01 M H_2SO_4 (flow rate: 0.8 mL min^{-1}). The method employed detected C2–C6 volatile fatty acids and the n- and iso-forms of C3–C6.

Other Analytical Parameters

The dry matter content was quantified by drying the biomass at 105°C overnight and weighing the residual material. Additional heating at 550°C gave the organic dry matter (oDM) content (Ács et al., 2015). pH was determined with a Radelkis OP-211/2 device equipped with an OP-0808P pH electrode.

VOA/TIC (Volatile organic acids/Total inorganic carbon) ratio was calculated with the use of a Pronova FOS/TAC 2000 Version 812-09.2008 automatic titrator.

The Metagenomic Sampling

A total of seven samples were investigated via IonTorrent whole genome sequencing and T-RFLP fingerprinting, which are compiled in **Table 1**.

Two additional sets of reactors were included in the metagenomic studies to better understand the long-term alterations in the microbial communities. The reactors, marked as CHw12 and CNw12 were run for 12 weeks similarly to an earlier long-term experimental arrangement (Szuhaj et al., 2016). The counterpart SHw12 and SNw12 fermentations were not included in the metagenomic analysis as the organic substrate was supplied only once at the start of the fermentations. This substrate was utilized during the first 14–16 days (**Figure 1**), after that period these reactors behaved as CNw12 and CHw12, respectively.

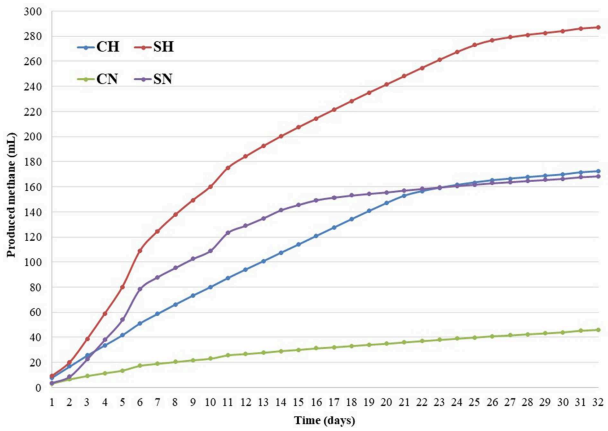

FIGURE 1 | Methane production in the batch reactors. Batch reactors were operated as described in Materials and Methods. The compositions of the reactors were: CN = biogas effluent, daily headspace replacement with nitrogen, CH = biogas effluent, daily headspace replacement with H_2, SN and SH = same as CN and CH, respectively, but supplied with α-cellulose substrate at the start. The long-term experiments were repetitions of the ones published in Szuhaj et al. (2016), that is why they are not reproduced here. The experimental errors of the triplicate samples are shown with the size of the symbols.

DNA Extraction

Whole genomic DNA was isolated from the pellet of 1.5 mL sample centrifuged at 13,000 rpm for 10 min. The CTAB (cetyl trimethylammonium bromide) based method was used as described previously (Ács et al., 2015). The separately isolated DNA samples from the parallel reactors were pooled together in an equal proportion to reach a final amount of 1 μg. These samples were used in the subsequent T-RFLP and metagenomic community analysis.

Terminal Restriction Fragment Length Polymorphism

PCR amplification (both in case of the community and the individual clones) and sequencing was conducted as described (Ács et al., 2013). Samples from biological replicates were pooled

for sequencing. The primer pair mcrA-F and mcrA-R (Luton et al., 2002) were used to detect the response of the methanogenic archaea to the H_2 addition with or without the organic substrate. The restriction endonucleases MboI and BstNI were used.

Ion Torrent Next Generation Sequencing and Data Evaluation

Sequencing

The genomic DNA samples were sequenced using IonTorrent PGM platform (Life Technologies, Thermo Scientific) according to the recommendations of the manufacturer. Fragment libraries were generated from the samples using Ion Xpress Plus Fragment Library Kit, Ion Shear Plus Reagents Kit was implemented for adapter ligation and nick translation. Platinum PCR SuperMix, ION Library TaqMan qPCR and Ion PGM 200 Xpress template kits were used for library amplification, quantification and for the emulsion PCR, respectively. Sequencing was performed on Ion 318 chips, generating 246,000–367,000 high quality reads per sample with an average read length of 215 ± 86 bp and good completeness of the rarefaction curves (**Supplementary Figure 2**).

Raw Sequence Filtering

Galaxy Europe server was employed to pre-process the raw sequences (https://usegalaxy.eu). Low-quality reads were filtered by Prinseq (min. length: 150; min. score: 15; quality score threshold to trim positions: 20; sliding window used to calculated quality score: 1) (Schmieder and Edwards, 2011). Quality of raw and filtered sequences were checked with FastQC program. The key quality parameters were as follows: node count 2,638, total length 12,027,501 bp, N50 4,947 bp, shortest node 2,000 bp.

Read-Based Metagenomics

Filtered high quality sequences were further analyzed by Diamond software, applying LCA (Lowest Common Ancestor) algorithm (Buchfink et al., 2014). Diamond parameters were set as follows: Blast Mode: BlastX, Reference database: NCBI nr database. MEGAN6 was used to add taxon names to Diamond sequence classifications (Min Score: 80, Min support percent: 80, Min support: 15, Min complexity filter: 0.3, LCA algorithm: weighted) (Huson et al., 2016).

Genome-Based Evaluation of the Sequencing Data

Filtered sequences produced by Prinseq were co-assembled using Megahit (Minimum contig length: 1,000 bp, Minimum k-mer size: 21, Maximum k-mer size 141) (D. Li et al., 2015). After simplifying the header of contig FASTA file, using the Anvi'o script, Bowtie2 was employed to map back the original sequences to the contigs (Langmead and Salzberg, 2012). Then we used Anvi'o V5 following the "metagenomics" workflow (Eren et al., 2015). Briefly, during the first step contig database was generated, where open reading frames were identified by Prodigal and each contig k-mer frequencies were computed. Hidden Markov Modell (HMM) of single-copy genes were aligned by HMMER (Finn et al., 2011; Campbell et al., 2013; Rinke et al., 2013; Simão et al., 2015). We used InterProScan v5.31-70 and the metagenome classifier Kaiju for functional and taxonomic annotation of contigs (Finn et al., 2014; Jones et al., 2014; Menzel et al., 2016; Agarwala et al., 2018). The outputs were imported into the contig database. BAM files made by Bowtie2 were used to profile contig database, this way sample-specific information was generated for the contigs (i.e., mean coverage). Three automated binning programs, namely CONCOCT, METABAT2, and MAXBIN2 were employed to reconstruct microbial genomes from the contigs (Minimum length: 2000) (Alneberg et al., 2013; Kang et al., 2015; Wu et al., 2016). We also used the Anvi'o human-guided binning and "anvi-refine" options (Delmont and Eren, 2018). The binning results were incorporated to the contig database.

RESULTS

Biomethane Production, Hydrogen Utilization, and Analytical Parameters

Five-weeks long experiments were conducted in order to reach the exhaustion of the CO_2 from the system. After start-up, the reactors showed increasing methane production. The control reactors (CN) produced 46.1 ± 1.4 mL (1.81 ± 0.05 mmol) CH_4, this could be accounted for the residual biogas potential present in the inoculum. The samples containing added α-cellulose (SN) produced 168.45 ± 3.73 mL (6.62 ± 0.15 mmol) CH_4 (**Figure 1**), i.e., nearly 100% conversation was achieved based upon the theoretical methane yield of the substrate (4.81 mmol, **Table 2**). The distinct kinetics of the SN (fed with α-cellulose) and CH (fed with H_2 + CO_2) samples, indicates that H_2 dissolution is more limiting than substrate degradation, although the total CH4 production was the same in this particular case. **Table 2** shows the predicted origin of methane produced in the reactors.

Analytical parameters (TS, oTS, VOA/TIC, pH, NH_4^+) were measured at the beginning and at the conclusion of each fermentation. Initial TS and oTS were 5.82 and 74%, respectively. After digestion these values dropped slightly to 5.41 and 71%. The VOA/TIC ratio remained below 0.2 and the ammonium ion concentrations were below 4 g L^{-1} throughout the experiments (data not shown). Due to the CO_2 consumption and the daily flushing of the head spaces with N_2, a strong shift from an initial value of pH 7.4 to around pH 8.5–9.4 was observed. This could have been compensated with CO_2 addition as demonstrated by Szuhaj et al. (2016) and others (Alimahmoodi and Mulligan, 2008; Salomoni et al., 2011; Lee et al., 2012; Garcia-Robledo et al., 2016).

The accumulation of organic acids was measured every week (**Figure 2**). The inoculum contained organic acids below the detection limit. A pronounced increase in the acetic acid and isovaleric acid contents was apparent after the first

TABLE 2 | Source of the produced methane (mmol).

Sample name	CN	SN	CH	SH
CH_4 from inoculum	1.81 ± 0.05	1.81 ± 0.05	1.81 ± 0.05	1.81 ± 0.05
CH_4 from substrate		4.81 ± 0.09		4.51 ± 0.09
CH_4 from H_2			4.96 ± 0.11	4.96 ± 0.11
Total	1.81 ± 0.05	6.62 ± 0.14	6.77 ± 0.16	11.28 ± 0.25

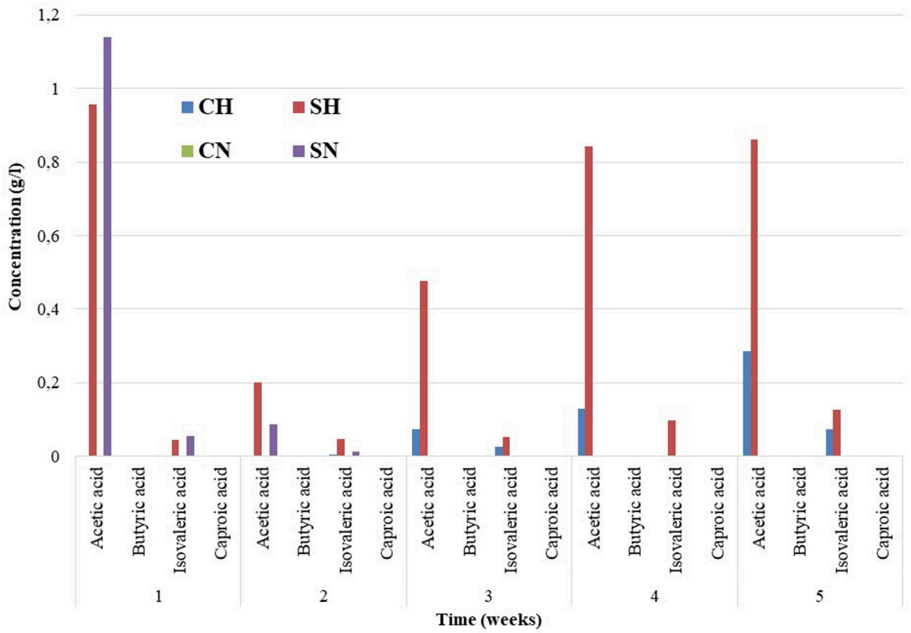

FIGURE 2 | Organic acid levels determined weekly in the reactors. The compositions of the reactors were as in **Figure 1**. The triplicate samples were pooled for the HPLC measurements. The long-term experiments were repetitions of the ones published in Szuhaj et al. (2016), that is why they are not reproduced here.

week in samples supplied initially with α-cellulose (SN and SH), which could be due to the rapid decomposition of the organic substrate and sluggish acetoclastic methanogenesis (Agneessens et al., 2018). The situation changed rapidly as the experiment continued and methanogens increased their activity and relative abundances. In the samples fed with H_2 a gradual accumulation of VFAs was observed in time. We assume that the alternative biochemical pathway, i.e., homoacetogenesis could be responsible for this observation (Sun et al., 2013; Angelidaki et al., 2018; Treu et al., 2018b).

T-RFLP Analysis of Archaeal *mcrA* Gene

In the T-RFLP of methanogens the primers primers designed for the gene coding for the large subunit of methyl-coenzyme M reductase (*mcrA*)were used. A total of 13 terminal restriction fragments (T-RFs) were generated, eight of which were reliably identified at genus level (**Table 3**). The remainders were apparently not detectable in the inoculum, which was used for the clone library preparation. The patterns of the samples were distinct and the shift in the microbial community was clearly visible (**Figure 3**). The genus *Methanosarcina* pre-dominated the inoculum, followed by *Methanoculleus* of around 40 and 28% relative abundances, respectively. The genera *Methanobacterium* and *Methanobrevibacter* were equally distributed in the inoculum sample (12%) followed by *Methanomassiliicoccus* and an unknown taxon. The methanogenic composition of samples CN and SN resembled that of the inoculum, although the proportions (especially the fragment at 223 bp, which we were not able to identify with full certainty, and at 254 bp—*Methanosarcina mazei*) were different, which is possibly due to the substrate change. In the T-RFLP pattern of CH, the predominance of the genus *Methanobacterium* at the expenses of the genera *Methanosarcina* and *Methanoculleus* was evident. The pattern of SH resembled that of CH. In this case three putative species of the genus *Methanobacterium* represented more than 78% of the community (Barret et al., 2013; Wintsche et al., 2016; Liu et al., 2018).

The diversity of sample CNw12 was strikingly low. *Methanobacterium* species were the most abundant archaea in this sample, which predominated the *Archaea* community from the early phase of the experiments. It is worth noting that the diversity in sample CHw12 was more pronounced than that of CNw12, containing five T-RFs of uncultured methanogens. Four of these were present in sample CH in comparable amounts. Apparently, the continuous H_2 and CO_2 input selected for a stable community capable of sustainable CH_4 production. This was in line with the previous observations (Szuhaj et al., 2016).

Alterations of the Microbiome Followed by Whole Metagenome Sequencing

The major taxonomical differences among the samples taken from the reactors subjected to various treatments (**Table 1**) were identified.

Clustering of the Metagenomes

For the grouping of samples, UPGMA (Unweighted Pair Group Method with Arithmetic Mean) was used, which refers to the entire microbial communities and indicates an average connection model. **Figure 4** shows that the microbial communities developed into well-separated lineages. The

TABLE 3 | Identified clones for the T-RFLP analysis.

Fragment length	Genus	Species	Identities	Gaps
50 bp	*Methanomassilicoccus*	*Luminyensis*	335/338 (99%)	0/338 (0%)
132 bp	*Methanoculleus*	*Bourgensis MS2T*	440/477 (92%)	6/477 (1%)
144 bp	*Methanoculleus*	*Bourgensis MAB1*	464/473 (98%)	0/473 (0%)
219 bp	*Methanobacterium*	*Petrolearium*	385/447 (86%)	5/447 (1%)
223 bp	*Methanobacterium*	*Ivanovii*	329/478 (69%)	21/478 (4%)
	Methanobrevibacter	*Millerae*	326/472 (69%)	6/472 (1%)
245 bp	*Methanosarcina*	*Mazei*	437/485 (90%)	0/485 (0%)
317 bp	Unknown	N/A	N/A	N/A
325 bp	Unknown	N/A	N/A	N/A
340 bp	Unknown	N/A	N/A	N/A
367 bp	Unknown	N/A	N/A	N/A
388 bp	*Methanobrevibacter*	*Gottschalkii*	417/470 (89%)	0/470 (0%)
417 bp	*Methanobacterium*	*Formicicum*	408/465 (88%)	2/465 (0%)
463 bp	Unknown	N/A	N/A	N/A

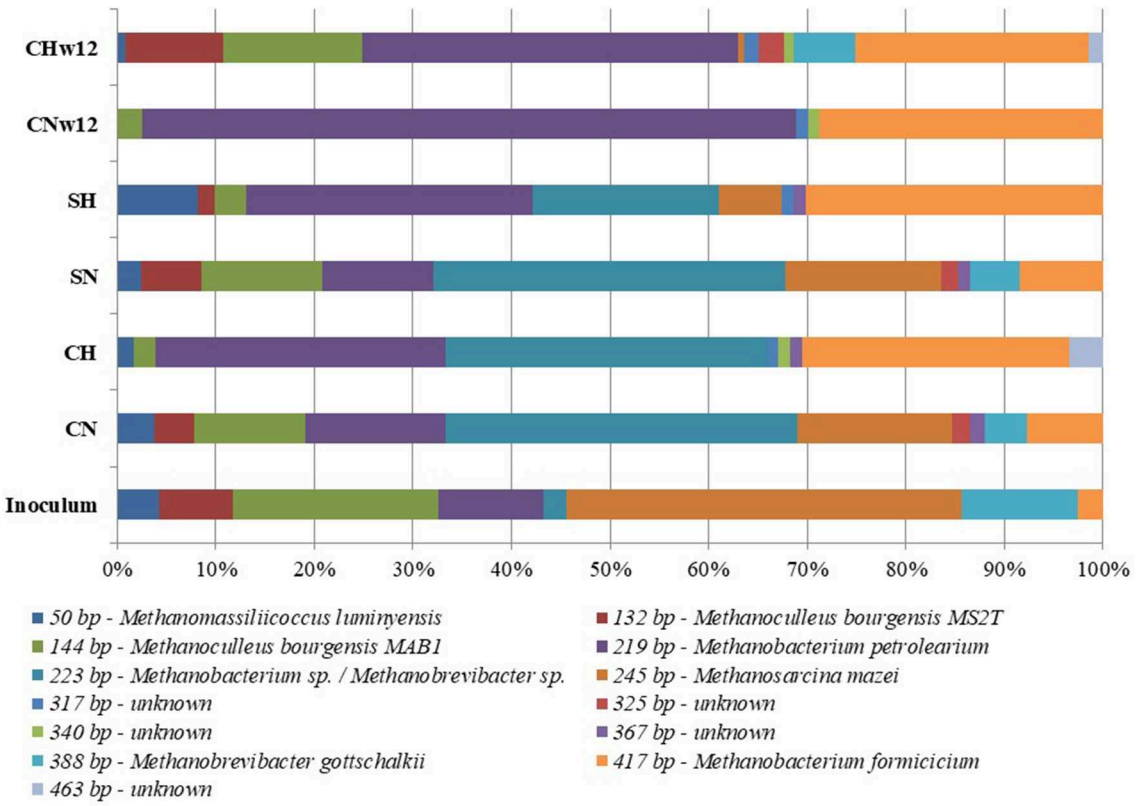

FIGURE 3 | Distribution of restriction patterns. Inoculum = biogas reactor effluent. The composition of the reactors were: CN = biogas effluent, daily headspace replacement with N_2, CH = biogas effluent, daily headspace replacement with H_2, SN and SH = same as CN and CH but supplied with α-cellulose substrate at the start. CNw12 = biogas effluent, daily headspace replacement with N_2 for 12 weeks, CHw12 biogas effluent, daily headspace replacement with $H_2 + CO_2$ for 12 weeks.

microbiota of the initial inoculum, originating from a biogas facility fed with silage and pig slurry, underwent a substantial rearrangement upon receiving daily supply of H_2 or N_2. An even more marked distinction can be observed between the microbiota of the bio-P2M reactors run for 4 and 12 weeks, respectively. The principal component analysis (**Supplementary Figure 1**) corroborated these conclusions, although in this test the CH, SH, and SN microbiomes mapped together and separated from CN.

The Bio-P2M Communities According to Read-Based Metagenome Analyses

Two general approaches were applied during the assessment of the taxonomical differences. On one hand, the abundances of the samples were compared to the inoculum at various taxonomic levels (pie diagrams presented in **Figure 6** and **Supplementary Figure 3**). On the other hand, the differential shifts in community composition were visualized relative to the corresponding control reactor as reference (**Figures 5**, **7** and **Supplementary Figure 4**), i.e., the percentile differences between the N_2-fed controls and their bio-P2M pairs, which received the $H_2 + CO_2$ stoichiometric gas mixture daily and, in the case of samples plotted in the red columns, a single dosage of α-cellulose at the start of the experiment. Hence, the horizontal columns may extend in either positive or negative directions. The taxa on the Y axes of these figures are arranged from top to down following their relative abundance in the inoculum.

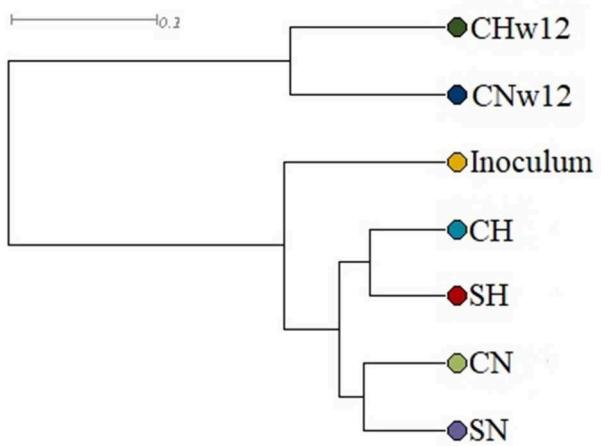

FIGURE 4 | UPGMA grouping of the samples. The compositions of the reactors were as in **Figure 3**.

Bacterial community

At phylum level only a few pronounced differences were observed among the fermenters subjected to different treatments (**Supplementary Figure 3**). Not surprisingly the long-term fermenters had the most distorted and least diverse communities compared to the inoculum.

In an attempt to visualize the microbial rearrangements as a result of H_2 (Sample CH) or substrate + H_2 (sample SH) addition, we plotted the differences relative to the corresponding controls, i.e., CN and SN, respectively (**Supplementary Figure 4**).

A relative expansion of *Firmicutes* could be noted at the expense of most other phyla. Their relative abundances did not change very much during the first 4 weeks of the operation of the bio-P2M reactors (59 ± 4%), but raised to 80 ± 1% upon sustained $H_2 + CO_2$ feeding (**Supplementary Figure 3**). The abundances of the phyla *Spirochaetes, Planctomycetes, Synergistetes*, and *Fibrobacteres* decreased in the CH samples but elevated in the CHw12 reactors, relative to their respective controls (**Supplementary Figure 4**). Although, these represented only a small part of the overall community (2–4%) in case of the short-term samples, and a more distinctive portion (10–13%) in the long-term samples (**Supplementary Figure 3**), their response to H_2 (and the subsequent CO_2) addition is noteworthy and warrant further investigation. The most outstanding changes took place in the candidate phylum *Cloacimonetes*. Although they also represented a small fraction within the communities (≤3%) (**Supplementary Figure 3**), their response to H_2 addition was very pronounced (**Supplementary Figure 4**). Their overall share decreased in the long-term bio-P2M experiments, but their relative abundance increased 15-fold in the CHw12 reactor relative to its CNw12 control.

A comprehensive list of the genera identified in the inoculum and the percentile changes in their relative abundances in the various samples are compiled in **Supplementary Table 1A**. 18 of these genera exceeded the threshold value of 1.0% abundance in the inoculum. They encompassed 72–77% of the

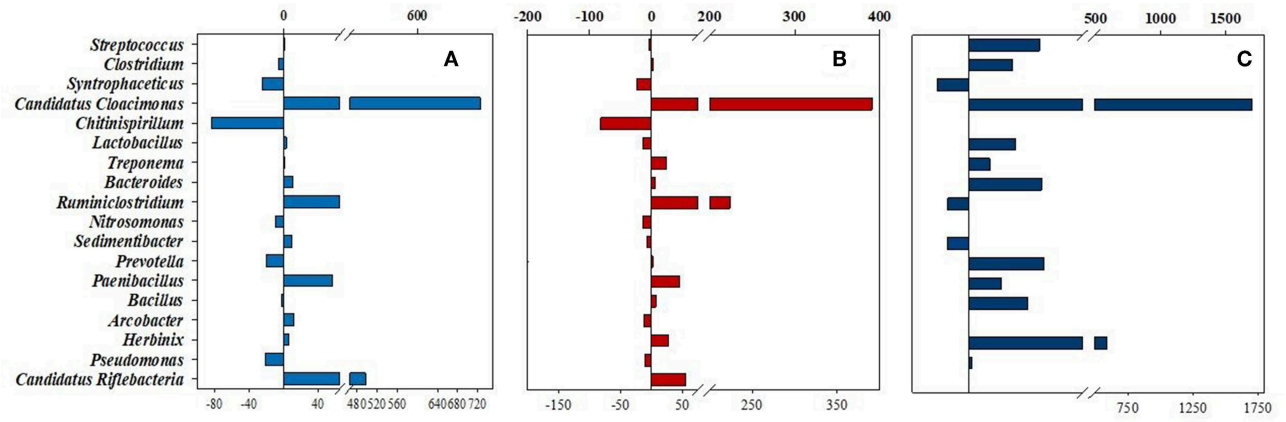

FIGURE 5 | Percentile changes of Bacteria relative abundances at genus level. The 18 genera, which were detected in >1% abundance. The changes between the reactors supplied with daily H_2 dose and their counterparts, flushed with N_2, are compared. **(A)** Light blue = CH-CN, **(B)** Red = SH-SN, and **(C)** Dark blue = CHw12-CNw12, respectively.

whole community. We focused our attention on this segment of the communities and their rearrangements under various operational conditions (**Table 4**).

Streptococcus species occurred frequently in all fermenters, their abundance, relative to the N_2-supplied controls changed substantially only in the long-term bio-P2M experiment (**Figure 5**). Likewise, the genus *Clostridium*, a well-known taxon of the microbiota in biogas reactors, were the second most abundant with increasing representation in the reactors running at balanced $H_2 + CO_2$ addition for an extended period of time. The less abundant genera *Lactobacillus*, *Treponema*, *Bacteroide*s, *Prevotella*, *Bacillus*, and particularly *Herbinix* behaved similarly. Long-term supply with $H_2 + CO_2$ apparently promoted the survival of these genera although they are not known to be able to metabolize these substrates except for some strains of the genera *Lactobacillus* and *Bacillus* (Koeck et al., 2014; Bohn et al., 2017). It is more likely that members of these genera survived by utilizing the biomass of the deceased other bacteria in the inoculum digestate. The opposite trend can be seen in the case of the genera *Syntrophaceticus*, *Ruminoclostridium*, *Sedimentibacter*, and *Candidatus Riflebacteria*. Others, like the genera *Paenibacillus*, *Arcobacter*, or *Pseudomonas* did not alter their representation as a result of $H_2 + CO_2$ feeding, consequently they may play negligible role in the bio-P2M conversion (**Figure 5**). The most pronounced change in abundance as a result of H_2-feeding was shown by the genus *Candidatus Cloacimonas*, which displayed a truly extraordinary abundance increase, relative to the controls containing N_2 in their headspace, both in our short term (7-fold see **Figure 5A**) or long term (17-fold see **Figure 5C**) bio-P2M experiments. Similar response was seen in the samples receiving α-cellulose substrate in addition to the gases **Figure 5B** and **Supplementary Table 1B**) indicating that the effect was primarily due to the addition of H_2. It is noteworthy, that their overall abundance decreased in time, i.e., from 5.34% in the inoculum to 1.02% in CHw12 and 0.06% in CNw12 (**Supplementary Tables 1A,B**), nevertheless their response to the sole addition of $H_2 + CO_2$ really deserves further attention (see Discussion).

TABLE 4 | Abundances of the eighteen major genera in the samples expressed as % of the total bacterial abundance.

Genus sample	Inoculum	CN	CH	SN	SH	CNw12	CHw12
	Abundance (%)						
Streptococcus	25.95	19.34	19.56	23.17	22.18	11.43	18.50
Clostridium	8.52	5.98	5.66	7.14	7.36	4.01	5.54
Syntrophaceticus	7.98	31.23	23.48	22.21	16.94	55.13	39.51
Candidatus cloacimonas	5.34	0.90	6.52	0.91	3.55	0.06	1.02
Chitinispirillum	2.96	0.97	0.16	1.00	0.18	0.00	0.00
Lactobacillus	2.76	1.74	1.79	1.94	1.67	0.46	0.64
Treponema	2.71	1.45	1.46	1.93	2.40	0.22	0.26
Bacteroides	2.51	2.10	2.33	2.36	2.51	0.76	1.25
Ruminiclostridium	2.16	2.66	5.74	2.10	4.71	2.12	1.72
Nitrosomonas	1.73	2.00	1.80	3.31	2.84	0.00	0.00
Sedimentibacter	1.63	0.94	1.03	1.18	1.09	0.30	0.24
Prevotella	1.38	1.29	1.03	1.07	1.09	0.25	0.41
Paenibacillus	1.32	0.56	0.87	0.71	1.02	0.69	0.89
Bacillus	1.27	0.96	0.94	0.76	0.82	0.60	0.91
Arcobacter	1.19	0.30	0.33	0.35	0.31	0.00	0.00
Herbinix	1.18	0.79	0.83	0.90	1.14	0.49	2.91
Pseudomonas	1.09	1.11	0.87	1.04	0.93	0.13	0.13
Candidatus riflebacteria	1.03	0.07	0.35	0.35	0.54	0.00	0.00
Σ Abundance (%)	72.71	74.38	74.76	72.42	71.26	76.66	73.95

Archaeal community

The representation of *Archaea* was low, ranging from 5.98 to 12.35% in the microbiome compared to *Bacteria* (88.91–94.01%). The *Archaea* content of the inoculum (9.28%) is typical for the mesophilic CSTR biogas communities (Pyzik et al., 2018). The overall representation of *Archaea* did not change considerable in our reactors except for a substantial loss in the long-term reactors supplied with N_2 (CNw12 = 5.98%) relative to the $H_2 + CO_2$-fed ones (CHw12 = 11.09%). Within this *Archaea* community 7 genera had relative abundance ≥0.5%. The distribution of these genera is presented in **Figure 6**. The pie chart is arranged similarly as in case of the *Bacteria*. A closer inspection on archaeal genera, compared to that of the inoculum (**Supplementary Table 1C**), revealed an overall decrease in the diversity. The genus *Methanobacterium* predominated the archaeal community in all reactors as well as in the inoculum, comprising 62–91% of all *Archaea* (**Figure 6**). In the long-term sample (CHw12) they encompassed the *Archaea* community almost exclusively. Their prevalence decreased considerably in CHw12 where the genus *Methanoculleu*s emerged in abundance (**Supplementary Table 1C**).

When the three fermentations receiving daily H_2 (and in one case CO_2) dosage (CH, SH, CHw12) were compared pairwise with their relevant controls, supplied with N_2 daily, an interesting picture emerged (**Figure 7**). The second most abundant genus in the inoculum, *Methanothrix* responded strongly to H_2 addition (**Figure 7A**) in the first part of the experiment with or without initial dosage of α-cellulose (**Figures 7A,B**), but the effect diminished in time (**Figure 7C**). Similarly to *Methanobacterium*, the genera *Methanosarcina* and *Methanothermobacter* did not change in their abundance much upon H_2 (and CO_2) injection in the headspace (**Supplementary Table 1C**). The hydrogenotrophic genera *Methanospirillum* and *Methanobrevibacter* apparently could not successfully sustain their life for an extended period of time when supplied with $H_2 + CO_2$. Contrary to all major *Archaea* genera, *Methanoculleus* effectively took advantage of long-term feeding solely with H_2+CO_2 and increased its abundance more than 11-fold (**Figure 7C**) relative to its control CNw12.

The Genome-Centric Bio-P2M Microbiomes

The sequencing data used above for read-based evaluation were subjected to genome-based analyses as well. Three automatic binning programs and Anvi'o human-guided binning option were tested (**Figure 8**). The bins obtained with these programs were basically similar with a few interesting features. 17

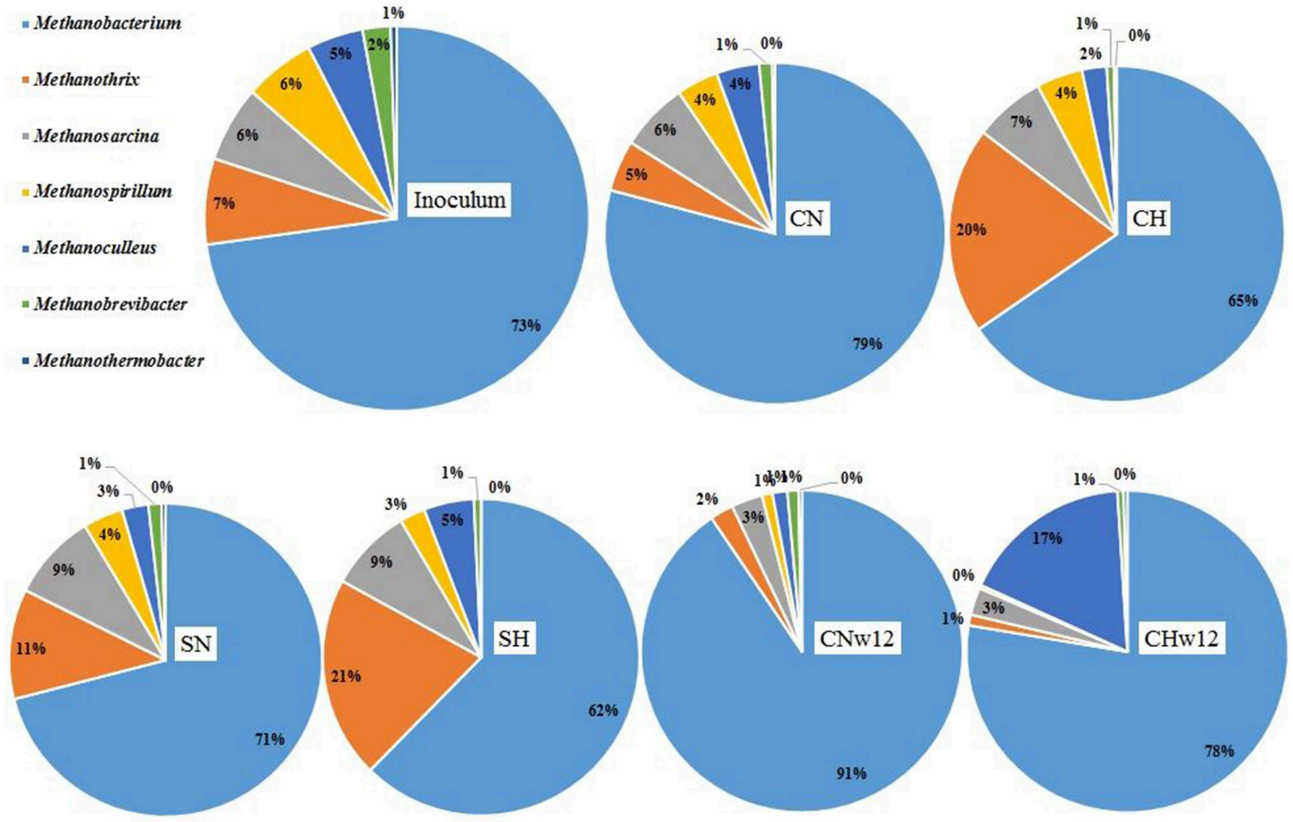

FIGURE 6 | Relative abundances of the Archaea genera. The compositions of the reactors were as in **Figure 3**.

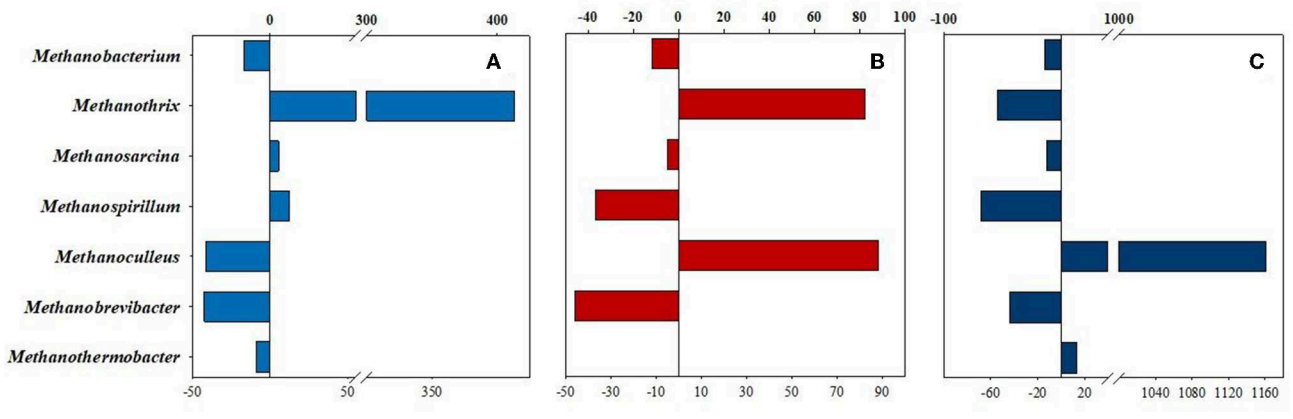

FIGURE 7 | Percentile changes of Archaea relative abundances at genus level. The changes between the reactors supplied with daily H_2 dose and their counterparts, flushed with nitrogen, are compared. **(A)** Light blue = CH-CN, **(B)** Red = SH-SN, and **(C)** Dark blue = CHw12-CNw12, respectively.

bins were constructed using the human-guided automated binning programs that rely on co-abundance of sequences as well as compositional information, such as GC content, tetranucleotide frequencies and identification of single-copy genes. Some of the bins had insufficient content at deep taxonomic resolution, e.g., Bins 1, 4, 10, 12, 14 (**Figure 8**). Others allowed the classification at phylum level, Bins 2 and 8 were linked to the phylum *Firmicutes*. In certain bins, a closer look allowed the recognition of the class *Clostridia* within *Firmicutes* (Bins 13 and 16). More interesting bins revealed their content at deeper taxonomic levels, such as the bacterial genera *Streptococcus* (Bin 6), *Caldicoprobacter*

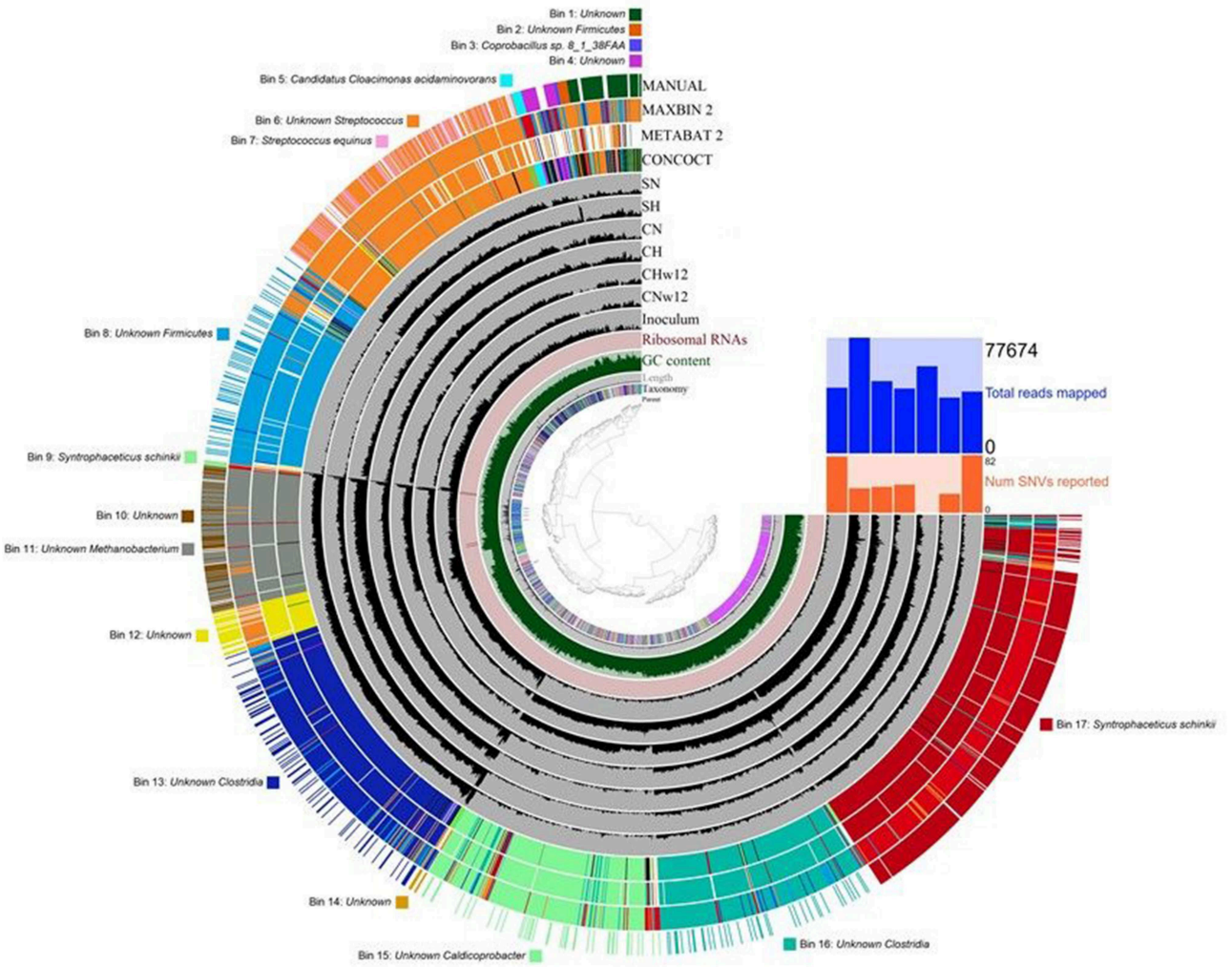

FIGURE 8 | Results of the genome-based evaluation (binning) of sequencing data. The dendogram in the center displays the hierarchical clustering of contigs based on their sequence compositions. The layers from inside out are as follows: (1) The parent layer marks the splits originated from the same contigs with gray bars. (2) The Kaiju taxonomic layer shows the taxonomy for each open reading frame detected in a given split. (3) The length layer indicates the actual length of a given split. (4) GC-content layer. (5) Ribosomal RNA layer. (6) Gray layers represent every sample and each black bar is the coverage of a given split in a given sample. (7) Colored layers: CONCOCT, MAXBIN 2, METABAT 2 display the results of these automated binning methods, respectively, and the MANUAL layer indicates the manual refinement of the automated binning results. The bins and the corresponding taxa are listed around the figure. The compositions of the reactors were as in **Figure 3**.

(Bin 15), and the methanogenic archaeal Bin 11 belonging to the genus *Methanobacterium*. Finally, the completion and low redundancy of certain bins made the identification available at species level, such as Bins 3, 5, 7, 9, and 17. In these cases the taxonomic resolutions were apparently better than that of the read-based evaluation (see section Bacterial Community) of the same sequencing data. *Coprobacillus sp. 8_1_38FAA* (Bin 3), *Streptococcus equinus* (Bin 7), *Syntrophaceticus schinkii* (Bins 9 and 17), and *Candidatus Cloacimonas acidaminovorans* (Bin 5) were clearly identified. The binning software constructed two separate bins containing *S. schinkii*, which may point to the presence of two separate subpopulations of this strain in the bio-P2M communities. The detailed summary of gene calls obtained in the genome-centric evaluation is compiled in **Supplementary Table 2**.

Discussion

The Response of the Bacterial and Archaeal Community to Bio-P2M Conditions

The feasibility of bio-P2M has been substantiated by several previous studies employing pure or enriched microbial communities (Martin et al., 2013; Bassani et al., 2015; Kougias et al., 2017b; Mulat et al., 2017; Rachbauer et al., 2017; Angelidaki et al., 2018; Aryal et al., 2018) and digestate (Szuhaj et al., 2016). In this study we have analyzed the adaptation of the microbial community of a mesophilic biogas plant effluent to become efficient catalyst of the bio-P2M process, i.e., to convert "excess green electricity" to bio-methane that is storable and transportable via the natural gas pipelines. The alterations of the "catalyst" microbial community during the first 4 weeks and sustained bio-P2M operation were followed in fed-batch

reactors receiving a daily dosage of H_2 + CO_2. Controls received N_2 gas. Significant and characteristic changes took place under the bio-P2M condition, which may contribute to the understanding of the microbial events and the ways to test, manage and control the complex microbial community for efficient function.

Members of the kingdom *Bacteria* were not expected to directly participate in the bio-P2M conversion. Nevertheless, they responded to the changing conditions. This could be due partly to starvation and partly to the successful interaction of some members of the *Bacteria* community with potential methanogenic *Archaea* partners.

The predominant genera in the inoculum were fairly well-preserved in the samples supplied daily with H_2 (+CO_2 in one case) or N_2 for various lengths of time, irrespective of supplementing the communities with an initial cellulosic substrate or not. The general bacterial community structure of the inoculum showed a high degree of similarity to other studies conducted from similar starting materials (Wirth et al., 2012; Stolze et al., 2015). The predominance of the phyla *Firmicutes, Proteobacteria*, and *Bacteroidetes* was apparent in previous investigations (Wirth et al., 2015; Rachbauer et al., 2017), similarly to the present study (**Supplementary Figure 3**). The general spread of *Firmicutes* could be seen at the expense of other phyla. This is not surprising since this phylum is the most common one in biogas fermenters, thanks to a great number of diverse representatives of the orders *Bacillales* and *Clostridiales*, capable of catalyzing various biochemical reactions, thus facilitating the easy adaptation to various environments (Aryal et al., 2018; Buettner and Noll, 2018; Treu et al., 2018a) Nevertheless, the selection for the phylum *Synergistetes* upon long-term exposure to H_2 + CO_2 is remarkable. *Synergistetes* have been implicated in syntrophic acetate oxidation (Hattori, 2008; Müller et al., 2013; Westerholm et al., 2016) whereas acetate accumulation took place in the bio-P2M reactors both in relatively short-term (**Figure 2**) and long-term (Szuhaj et al., 2016) operation suggesting the shift of equilibrium toward homoacetogenesis.

As we refined the search to genus level, *Streptococcus* emerged being the predominant genus with around 11–25% share in the community (**Table 4**). They likely originated from the ensilaged substrate used at the biogas plant providing the inoculum (McDonald, 1982; Kampmann et al., 2014; Bohn et al., 2017).

The genera *Clostridium*, *Syntrophaceticus*, and *Candidatus Cloacimonas* were among the frequent taxa. H_2 facilitated the prevalence of *Candidatus Cloacimonas acidaminovorans* up to 17-fold relative to the N_2-fed controls (**Figure 5**). This candidate strain was reconstructed and thoroughly characterized via metagenomics sequencing and metaproteome analysis (Pelletier et al., 2008). It is assumed to be involved in syntrophic oxidation of propionate (Li et al., 2014) and contains a full set of genes coding for at least one "Fe-only hydrogenase" (Pelletier et al., 2008). This "Fe-only hydrogenase," encoded by the *hymABC* structural and the *hydEFG* accessory genes, is in fact probably a [FeFe]-hydrogenase (Degli Esposti et al., 2016), which is frequently found in anaerobic prokaryotes. "Fe-only hydrogenase" was detected so far only in *Archaea* (Lubitz et al., 2014) and is intimately linked to methanogenesis. [FeFe]-hydrogenases typically function *in vivo* in the H_2 evolution direction, which is not required in the bio-P2M reactor supplied semi-continuously with H_2 gas. In addition, syntrophic oxidation of volatile fatty acids is thermodynamically only favorable under very low H_2 partial pressure (Schnürer et al., 1999), whereas in our system the conditions apparently prefer the opposite reaction, i.e., homoacetogenesis. These considerations cannot explain the dramatic, H_2-induced abundance of *Candidatus Cloacimonas* in our bio-P2M reactors. The rationalization of this observation remains puzzling. Members of the other long-term survivor genus *Herbinix* (**Figure 5** and **Supplementary Table 1A**) so far have been isolated from thermophilic AD reactors (Koeck et al., 2014; Pap et al., 2015).

The presence of *Prevotella* species in swine manure has been demonstrated (Cook et al., 2010; Park et al., 2014), therefore they might have originated from the swine slurry component of the inoculum.

The seven methanogenic genera encompass 97–99% of all *Archaea* detected in the bio-P2M reactors (**Figure 6**). All of them are either hydrogenotrophic methanogens or capable of the hydrogenotrophic lifestyle (genus *Methanosarcina*). This is not very surprising in light of the operating conditions prevailing in the bio-P2M reactors. Their distinctly different response to the addition of H_2 + CO_2, however, was surprising. The genus *Methanobacterium* covered the bulk of *Archaea* (**Figure 6**) like in trickle-bed (Rachbauer et al., 2017) or batch reactors (Wahid et al., 2019). During the long-term bio-P2M operation only the genus *Methanoculleus* responded positively by increasing its relative abundance relative to the N_2-fed controls (**Figure 7** and **Supplementary Table 1C**) corroborating earlier findings about outstanding performance of this genus in bio-P2M (Kougias et al., 2017a; Angelidaki et al., 2018; Treu et al., 2018a). It is tempting to speculate that either *Methanoculleus* is capable of fully supporting its survival and activity independently from the rest of the AD *Bacteria* and *Archaea* community, or *Methanoculleus* developed some sort of syntrophic relationship with *Candidatus Cloacimonas* to support their continued existence. The stagnation or decreasing relative abundances of the other methanogenic genera (**Figure 7C**) might indicate that they cannot function well when only H_2 + CO_2 is available for them.

The relationship between the observed alterations in the community and the relevance of these phenomena to the operational stability of the bio-P2M microbial community should be understood in future explorations.

Comparison of the T-RFLP Data With NGS Results

In addition to the similarities, the comparison of the datasets obtained from the two approaches revealed some differences due to the distinct methodologies. One possible explanation for the discrepancies might be the PCR amplification bias inherent in the T-RFLP technique

(Sipos et al., 2007; Schütte et al., 2008). An additional predisposition may arise from the equivocality of the analysis of the sequences. For example, the *mcrA* genes of *Methanobacterium* and *Methanothermobacter* have very similar sequences. Using the NCBI database the clone RF 223 bp was identified both as *Methanobacterium petrolerium* and *Methanothermobacter thermautotrophicus* strains. Finally, on-line libraries containing sufficient quantities of accurate *mcrA* sequences are still in development and one needs to take into account that the targeted sequence length was rather small (∼500 bp).

Nevertheless, strong similarities between the results of the two methodological approaches are worth noting. These are as follows: (i) The reduction of diversity, particularly in the long-term experiments, relative to the inoculum is apparent form both sets of data (**Figures 3**, **7**). (ii) The genus *Methanobacterium* predominated the archaeal community according to both T-RFLP and metagenome sequencing. Moreover, the genome-centric metagenome evaluation identified one *Archaea* bin (Bin 11), which belonged to "unknown *Methanobacterium*." (iii) All methanogenic T-RFLP clones, except for the methylotrophic *Methanomassiliicoccus* (RF 50 bp), found their corresponding metagenomics genera in the read-based metagenome analysis. A similar T-RFLP community was found in the work of Ziganshin et al. (2016).

Taken together, we concluded that the results provided by the two methods mutually validated each other, although the NGS data resulted in a more precise picture of the actual microbial community at genus level.

CONCLUSIONS

This study confirmed the technological feasibility and efficacy of the biological route of the P2M process using a complex and inexpensive microbial community as catalyst. The alterations in the community, originated from a regular mesophilic biogas plant effluent, were followed for an extended time period with or without supplementing the discontinuous H_2 (and CO_2) dosage with a single initial dose of organic substrate. We employed T-RFLP and shotgun metagenome sequencing techniques to monitor the changes in the community composition. The organic substrate did modify the community structure, but the bio-P2M process could be carried out without added organic substrate for an extended period of time. We highlighted interesting taxonomical and abundance shifts. Although H_2 (and/or CO_2) is not expected to influence the growth of *Bacteria*, marked changes took place in this part of the community. These were presumably due to varying survival strategies and capabilities of the taxa. Although the outstanding genus *Candidatus Cloacimonas* was not among the most abundant taxa, immensely preferred H_2 over N_2 in the reactors. Major modification in the methanogenic archaeal community took place. The abundant genera were all capable of performing hydrogenotrophic methanogenesis, but only the genus *Methanoculleus* found the bio-P2M conditions beneficial in the long run. Further studies are required, preferably at a larger scale and in continuous mode of operation to better understand and optimize the exact process conditions and parameters.

We proposed an alternative, economically and technologically feasible way to integrate the bio-P2M technology into biogas production schemes by using the microbial community of the effluent from biogas plants on site. The findings substantiate that the surplus renewable H_2 is efficiently handled by the mixed anaerobic microbes from the biogas reactor, offering an additional valorization possibility for the biogas plants.

DATA AVAILABILITY STATEMENT

The datasets generated for this study can be found on SRA under the code PRJNA562179. Link: https://www.ncbi.nlm.nih.gov/bioproject/PRJNA562179. The T-RFLP sequences are attached as **Supplementary Table 3**.

AUTHOR CONTRIBUTIONS

KK conceived the study, participated in its design and evaluation. NÁ and MS carried out the bio-P2M experiments, T-RFLP and took part in the evaluation of NGS data. GM and RW performed the Ion Torrent Sequencing and analyzed the metagenomic data. KK, NÁ, ZB, and GR composed the manuscript. All the authors agreed in publishing the final version of this paper.

FUNDING

This study has been supported in part by the Hungarian National Research, Development and Innovation Fund projects GINOP-2.3.2-15-2016-00011, GINOP-2.2.1-15-2017-00081, GINOP-2.2.1-15-2017-00033, and EFOP-3.6.2-16-2017-00010. RW, ZB, and GM received support from the Hungarian NKFIH fund projects PD121085, FK123902, and FK123899 financed under the OTKA PD16 and FK 16 funding schemes. This work was also supported by the János Bolyai Research Scholarship (for GM) of the Hungarian Academy of Sciences.

SUPPLEMENTARY MATERIAL

The Supplementary Material for this article can be found online at: https://www.frontiersin.org/articles/10.3389/fenrg.2019.00132/full#supplementary-material

Supplementary Figure 1 | Principle coordinate analysis on the sequenced samples.

Supplementary Figure 2 | Rarefaction curve showing adequate sequencing depth for effective taxonomical resolution.

Supplementary Figure 3 | Relative abundances of the Bacteria phyla. The compositions of the reactors were as in **Figure 3**.

Supplementary Figure 4 | Percentile changes of Bacteria relative abundances at phylum level. The changes between the reactors supplied with daily H_2 dose and

their counterparts, flushed with N_2, are compared. Light blue = CH-CN, Red = SH-SN, and Dark blue = CHw12-CNw12, respectively.

Supplementary Table 1A | Percentile changes in the abundances of Bacteria genera compared to the inoculum. Color codes are indicated at the top of the right-side column.

Supplementary Table 1B | Below the bar (<1% abundance in the inoculum) Bacteria genera in the samples fed daily with H_2 (+CO_2), compared to their relevant controls supplied daily with N_2 only. Color codes are indicated at the top of the right-side column.

Supplementary Table 1C | Percentile changes in Archaea genera abundances compared to the inoculum. Color codes are indicated at the bottom of the table.

Supplementary Table 2 | Gene calls of the genome-based evaluation.

Supplementary Table 3 | The T-RFLP clone sequences.

REFERENCES

Ács, N., Bagi, Z., Rákhely, G., Minárovics, J., Nagy, K., and Kovács, K. L. (2015). Bioaugmentation of biogas production by a hydrogen-producing bacterium. *Bioresour. Technol.* 186, 286–293. doi: 10.1016/j.biortech.2015.02.098

Ács, N., Kovács, E., Wirth, R., Bagi, Z., Strang, O., Herbel, Z., et al. (2013). Changes in the Archaea microbial community when the biogasfermenters are fed with protein-rich substrates. *Bioresour. Technol.* 131, 1121–1127. doi: 10.1016/j.biortech.2012.12.134

Agarwala, R., Barrett, T., Beck, J., Benson, D. A., Bollin, C., Bolton, E., et al. (2018). Database resources of the National Center for Biotechnology Information. *Nucleic Acids Res.* 46, D8–D13. doi: 10.1093/nar/gkx1095

Agneessens, L. M., Ottosen, L. D. M., Andersen, M., Berg Olesen, C., Feilberg, A., and Kofoed, M. V. W. (2018). Parameters affecting acetate concentrations during *in-situ* biological hydrogen methanation. *Bioresour. Technol.* 258, 33–40. doi: 10.1016/j.biortech.2018.02.102

Alimahmoodi, M., and Mulligan, C. N. (2008). Anaerobic bioconversion of carbon dioxide to biogas in an upflow anaerobic sludge blanket reactor. *J. Air Waste Manage. Assoc.* 58, 95–103. doi: 10.3155/1047-3289.58.1.95

Alneberg, J., Bjarnason, B. S., de Bruijn, I., Schirmer, M., Quick, J., Ijaz, U. Z., et al. (2013). *CONCOCT*: *Clustering cONtigs on COverage and ComposiTion*, 1–28. Available online at: http://arxiv.org/abs/1312.4038.

Angelidaki, I., Treu, L., Tsapekos, P., Luo, G., Campanaro, S., Wenzel, H., et al. (2018). Biogas upgrading and utilization: current status and perspectives. *Biotechnol. Adv.* 36, 452–466. doi: 10.1016/j.biotechadv.2018.01.011

Aryal, N., Kvist, T., Ammam, F., Pant, D., and Ottosen, L. D. M. (2018). An overview of microbial biogas enrichment. *Bioresour. Technol.* 264, 359–369. doi: 10.1016/j.biortech.2018.06.013

Bagi, Z., Ács, N., Bálint, B., Horváth, L., Dobó, K., Perei, K. R., et al. (2007). Biotechnological intensification of biogas production. *Appl. Microbiol. Biotechnol.* 76, 473–482. doi: 10.1007/s00253-007-1009-6

Barret, M., Gagnon, N., Kalmokoff, M. L., Topp, E., Verastegui, Y., Brooks, S. P. J., et al. (2013). Identification of Methanoculleus spp. as active methanogens during anoxic incubations of swine manure storage tank samples. *Appl. Environ. Microbiol.* 79, 424–33. doi: 10.1128/AEM.02268-12

Bassani, I., Kougias, P. G., Treu, L., and Angelidaki, I. (2015). Biogas upgrading via hydrogenotrophic methanogenesis in two-stage continuous stirred tank reactors at mesophilic and thermophilic conditions. *Environ. Sci. Technol.* 49, 12585–12593. doi: 10.1021/acs.est.5b03451

Bohn, J., Yüksel-Dadak, A., Dröge, S., and König, H. (2017). Isolation of lactic acid-forming bacteria from biogas plants. *J. Biotechnol.* 244, 4–15. doi: 10.1016/j.jbiotec.2016.12.015

Buchfink, B., Xie, C., and Huson, D. H. (2014). Fast and sensitive protein alignment using DIAMOND. *Nat. Methods* 12, 59–60. doi: 10.1038/nmeth.3176

Buettner, C., and Noll, M. (2018). Differences in microbial key players in anaerobic degradation between biogas and sewage treatment plants. *Int. Biodeterior. Biodegradation* 133, 124–132. doi: 10.1016/j.ibiod.2018.06.012

Campbell, J. H., O'Donoghue, P., Campbell, A. G., Schwientek, P., Sczyrba, A., Woyke, T., et al. (2013). UGA is an additional glycine codon in uncultured SR1 bacteria from the human microbiota. *Proc. Natl. Acad. Sci. U.S.A.* 110, 5540–5545. doi: 10.1073/pnas.1303090110

Cook, K. L., Rothrock, M. J., Lovanh, N., Sorrell, J. K., and Loughrin, J. H. (2010). Spatial and temporal changes in the microbial community in an anaerobic swine waste treatment lagoon. *Anaerobe* 16, 74–82. doi: 10.1016/j.anaerobe.2009.06.003

Degli Esposti, M., Cortez, D., Lozano, L., Rasmussen, S., Nielsen, H. B., and Martinez Romero, E. (2016). Alpha proteobacterial ancestry of the [Fe-Fe]-hydrogenases in anaerobic eukaryotes. *Biol. Direct* 11:34. doi: 10.1186/s13062-016-0136-3

Delmont, T. O., and Eren, E. M. (2018). Linking pangenomes and metagenomes: the prochlorococcus metapangenome. *PeerJ* 2018, 1–23. doi: 10.7717/peerj.4320

Eren, A. M., Esen, O. C., Quince, C., Vineis, J. H., Morrison, H. G., Sogin, M. L., et al. (2015). Anvi'o: an advanced analysis and visualization platformfor'omics data. *PeerJ* 2015, 1–29. doi: 10.7717/peerj.1319

Finn, R. D., Bateman, A., Clements, J., Coggill, P., Eberhardt, R. Y., Eddy, S. R., et al. (2014). Pfam: the protein families database. *Nucleic Acids Res.* 42, 222–230. doi: 10.1093/nar/gkt1223

Finn, R. D., Clements, J., and Eddy, S. R. (2011). HMMER web server: interactive sequence similarity searching. *Nucleic Acids Res.* 39, 29–37. doi: 10.1093/nar/gkr367

Garcia-Robledo, E., Ottosen, L. D. M., Voigt, N. V., Kofoed, M. W., and Revsbech, N. P. (2016). Micro-scale H_2-CO_2 dynamics in a hydrogenotrophic methanogenic membrane reactor. *Front. Microbiol.* 7:276. doi: 10.3389/fmicb.2016.01276

Hattori, S. (2008). Syntrophic acetate-oxidizing microbes in methanogenic environments. *Microbes Environ.* 23, 118–127. doi: 10.1264/jsme2.23.118

Huson, D. H., Beier, S., Flade, I., Górska, A., El-Hadidi, M., Mitra, S., et al. (2016). MEGAN Community edition–interactive exploration and analysis of large-scale microbiome sequencing data. *PLoS Comput. Biol.* 12:e1004957. doi: 10.1371/journal.pcbi.1004957

Jones, P., Binns, D., Chang, H. Y., Fraser, M., Li, W., McAnulla, C., et al. (2014). InterProScan 5: genome-scale protein function classification. *Bioinformatics* 30, 1236–1240. doi: 10.1093/bioinformatics/btu031

Kampmann, K., Ratering, S., Geißler-Plaum, R., Schmidt, M., Zerr, W., and Schnell, S. (2014). Changes of the microbial population structure in an overloaded fed-batch biogas reactor digesting maize silage. *Bioresour. Technol.* 174, 108–117. doi: 10.1016/j.biortech.2014.09.150

Kang, D. D., Froula, J., Egan, R., and Wang, Z. (2015). MetaBAT, an efficient tool for accurately reconstructing single genomes from complex microbial communities. *PeerJ* 2015, 1–15. doi: 10.7717/peerj.1165

Koeck, D. E., Wibberg, D., Maus, I., Winkler, A., Albersmeier, A., Zverlov, V. V., et al. (2014). First draft genome sequence of the amylolytic *Bacillus thermoamylovorans* wild-type strain 1A1 isolated from a thermophilic biogas plant. *J. Biotechnol.* 192, 154–155. doi: 10.1016/j.jbiotec.2014.09.017

Kougias, P. G., Campanaro, S., Treu, L., Zhu, X., and Angelidaki, I. (2017a). A novel archaeal species belonging to *Methanoculleus genus* identified via *de-novo* assembly and metagenomic binning process in biogas reactors. *Anaerobe* 46, 23–32. doi: 10.1016/j.anaerobe.2017.02.009

Kougias, P. G., Treu, L., Benavente, D. P., Boe, K., Campanaro, S., and Angelidaki, I. (2017b). *Ex-situ* biogas upgrading and enhancement in different reactor systems. *Bioresour. Technol.* 225, 429–437. doi: 10.1016/j.biortech.2016.11.124

Kovács, K. L., Ács, N., Kovács, E., Wirth, R., Rákhely, G., Strang, O., et al. (2013). Improvement of biogas production by bioaugmentation. *Biomed Res. Int.* 2013:7. doi: 10.1155/2013/482653

Langmead, B., and Salzberg, S. L. (2012). Fast gapped-read alignment with Bowtie 2. *Nat. Methods* 9, 357–359. doi: 10.1038/nmeth.1923

Lee, J. C., Kim, J. H., Chang, W. S., and Pak, D. (2012). Biological conversion of CO_2 to CH_4 using hydrogenotrophic methanogen in a fixed bed reactor. *J. Chem. Technol. Biotechnol.* 87, 844–847. doi: 10.1002/jctb.3787

Lewandowska-Bernat, A. (2017). Opportunities of power-to-gas technology. *Energy Procedia* 105, 4569–4574. doi: 10.1016/j.egypro.2017.03.982

Li, D., Liu, C. M., Luo, R., Sadakane, K., and Lam, T. W. (2015). MEGAHIT: an ultra-fast single-node solution for large and complex metagenomics assembly via succinct de Bruijn graph. *Bioinformatics* 31, 1674–1676. doi: 10.1093/bioinformatics/btv033

Li, Y. F., Chen, P. H., and Yu, Z. (2014). Spatial and temporal variations of microbial community in a mixed plug-flow loop reactor fed with dairy manure. *Microb. Biotechnol.* 7, 332–346. doi: 10.1111/1751-7915.12125

Liu, C., Wachemo, A. C., Tong, H., Shi, S., Zhang, L., Yuan, H., et al. (2018). Biogas production and microbial community properties during anaerobic digestion of corn stover at different temperatures. *Bioresour. Technol.* 261, 93–103. doi: 10.1016/j.biortech.2017.12.076

Lubitz, W., Ogata, H., Ru, O., and Reijerse, E. (2014). Hydrogenases. *Chem. Rev.* 114, 4081–4148. doi: 10.1021/cr4005814

Luton, P. E., Wayne, J. M., Sharp, R. J., and Riley, P. W. (2002). The mcrA gene as an alternative to 16S rRNA in the phylogenetic analysis of methanogen populations in landfill. *Microbiology* 148, 3521–30. doi: 10.1099/00221287-148-11-3521

Martin, M. R., Fornero, J. J., Stark, R., Mets, L., and Angenent, L. T. (2013). A single-culture bioprocess of methanothermobacter thermautotrophicus to upgrade digester biogas by CO_2-to-CH_4 conversion with H_2. *Archaea* 2013:157529. doi: 10.1155/2013/157529

Mazza, A., Bompard, E., and Chicco, G. (2018). Applications of power to gas technologies in emerging electrical systems. *Renew. Sustain. Energy Rev.* 92, 794–806. doi: 10.1016/j.rser.2018.04.072

McDonald, P. (1982). Silage fermentation. *Trends Biochem. Sci.* 7, 164–166. doi: 10.1016/0968-0004(82)90127-X

Menzel, P., Ng, K. L., and Krogh, A. (2016). Fast and sensitive taxonomic classification for metagenomics with Kaiju. *Nat. Commun.* 7, 1–9. doi: 10.1038/ncomms11257

Mulat, D. G., Mosbæk, F., Ward, A. J., Polag, D., Greule, M., Keppler, F., et al. (2017). Exogenous addition of H_2 for an *in situ* biogas upgrading through biological reduction of carbon dioxide into methane. *Waste Manag.* 68, 146–156. doi: 10.1016/j.wasman.2017.05.054

Müller, B., Sun, L., and Schnürer, A. (2013). First insights into the syntrophic acetate-oxidizing bacteria–a genetic study. *Microbiol. Open* 2, 35–53. doi: 10.1002/mbo3.50

Nap, J. P., Bekkering, J., Hofstede, G., Faber, F., Wedema, R., Zwart, K., et al. (2019). *Biomethane from Hydrogen and Carbon Dioxide*. Hanze University of Applied Sciences. Available online at: https://research.hanze.nl/files/26384228/019_043_Bio_P2G_Boekje_22_2564_.pdf

Nzila, A. (2017). Mini review: update on bioaugmentation in anaerobic processes for biogas production. *Anaerobe* 46, 3–12. doi: 10.1016/j.anaerobe.2016.11.007

Pap, B., Györkei, Á., Boboescu, I. Z., Nagy, I. K., Bíró, T., Kondorosi, É., et al. (2015). Temperature-dependent transformation of biogas-producing microbial communities points to the increased importance of hydrogenotrophic methanogenesis under thermophilic operation. *Bioresour. Technol.* 177, 375–380. doi: 10.1016/j.biortech.2014.11.021

Park, S.-J., Kim, J., Lee, J.-S., Rhee, S.-K., and Kim, H. (2014). Characterization of the fecal microbiome in different swine groups by high-throughput sequencing. *Anaerobe* 28, 157–162. doi: 10.1016/j.anaerobe.2014.06.002

Pelletier, E., Kreimeyer, A., Bocs, S., Rouy, Z., Gyapay, G., Chouari, R., et al. (2008). "Candidatus Cloacamonas acidaminovorans": genome sequence reconstruction provides a first glimpse of a new bacterial division. *J. Bacteriol.* 190, 2572–2579. doi: 10.1128/JB.01248-07

Pyzik, A., Ciezkowska, M., Krawczyk, P. S., Sobczak, A., Drewniak, L., Dziembowski, A., et al. (2018). Comparative analysis of deep sequenced methanogenic communities: identification of microorganisms responsible for methane production. *Microb. Cell Fact.* 17:197. doi: 10.1186/s12934-018-1043-3

Rachbauer, L., Beyer, R., Bochmann, G., and Fuchs, W. (2017). Characteristics of adapted hydrogenotrophic community during biomethanation. *Sci. Total Environ.* 595, 912–919. doi: 10.1016/j.scitotenv.2017.03.074

Rinke, C., Schwientek, P., Sczyrba, A., Ivanova, N. N., Anderson, I. J., Cheng, J. F., et al. (2013). Insights into the phylogeny and coding potential of microbial dark matter. *Nature* 499, 431–437. doi: 10.1038/nature12352

Salomoni, C., Caputo, A., Bonoli, M., Francioso, O., Rodriguez-Estrada, M. T., and Palenzona, D. (2011). Enhanced methane production in a two-phase anaerobic digestion plant, after CO_2 capture and addition to organic wastes. *Bioresour. Technol.* 102, 6443–6448. doi: 10.1016/j.biortech.2011.03.079

Schmieder, R., and Edwards, R. (2011). Quality control and preprocessing of metagenomic datasets. *Bioinformatics* 27, 863–864. doi: 10.1093/bioinformatics/btr026

Schnürer, A., Zellner, G., and Svensson, B. H. (1999). Mesophilic syntrophic acetate oxidation during methane formation in biogas reactors. *FEMS Microbiol. Ecol.* 29, 249–261. doi: 10.1016/S0168-6496(99)00016-1

Schütte, U. M. E., Abdo, Z., Bent, S. J., Shyu, C., Williams, C. J., Pierson, J. D., et al. (2008). Advances in the use of terminal restriction fragment length polymorphism (T-RFLP) analysis of 16S rRNA genes to characterize microbial communities. *Appl. Microbiol. Biotechnol.* 80, 365–80. doi: 10.1007/s00253-008-1565-4

Simão, F. A., Waterhouse, R. M., Ioannidis, P., Kriventseva, E. V., and Zdobnov, E. M. (2015). BUSCO: assessing genome assembly and annotation completeness with single-copy orthologs. *Bioinformatics* 31, 3210–3212. doi: 10.1093/bioinformatics/btv351

Sipos, R., Székely, A. J., Palatinszky, M., Révész, S., Márialigeti, K., and Nikolausz, M. (2007). Effect of primer mismatch, annealing temperature and PCR cycle number on 16S rRNA gene-targetting bacterial community analysis. *FEMS Microbiol. Ecol.* 60, 341–350. doi: 10.1111/j.1574-6941.2007.00283.x

Stolze, Y., Zakrzewski, M., Maus, I., Eikmeyer, F., Jaenicke, S., Rottmann, N., et al. (2015). Comparative metagenomics of biogas-producing microbial communities from production-scale biogas plants operating under wet or dry fermentation conditions. *Biotechnol. Biofuels* 8:14. doi: 10.1186/s13068-014-0193-8

Sun, L., Müller, B., and Schnürer, A. (2013). Biogas production from wheat straw: Community structure of cellulose-degrading bacteria. *Energy. Sustain. Soc.* 3, 1–11. doi: 10.1186/2192-0567-3-15

Szuhaj, M., Ács, N., Tengölics, R., Bodor, A., Rákhely, G., Kovács, K. L., et al. (2016). Conversion of H_2 and CO_2 to CH_4 and acetate in fed-batch biogas reactors by mixed biogas community: a novel route for the power-to-gas concept. *Biotechnol. Biofuels* 9:102. doi: 10.1186/s13068-016-0515-0

Treu, L., Campanaro, S., Kougias, P. G., Sartori, C., Bassani, I., and Angelidaki, I. (2018a). Hydrogen-fueled microbial pathways in biogas upgrading systems revealed by genome-centric metagenomics. *Front. Microbiol.* 9:1079. doi: 10.3389/fmicb.2018.01079

Treu, L., Kougias, P. G., de Diego-Díaz, B., Campanaro, S., Bassani, I., Fernández-Rodríguez, J., et al. (2018b). Two-year microbial adaptation during hydrogen-mediated biogas upgrading process in a serial reactor configuration. *Bioresour. Technol.* 264, 140–147. doi: 10.1016/j.biortech.2018.05.070

Wahid, R., Mulat, D. G., Gaby, J. C., and Horn, S. J. (2019). Effects of H_2:CO_2 ratio and H_2 supply fluctuation on methane content and microbial community composition during *in-situ* biological biogas upgrading. *Biotechnol. Biofuels* 12, 1–15. doi: 10.1186/s13068-019-1443-6

Westerholm, M., Moestedt, J., and Schnürer, A. (2016). Biogas production through syntrophic acetate oxidation and deliberate operating strategies for improved digester performance. *Appl. Energy* 179, 124–135. doi: 10.1016/j.apenergy.2016.06.061

Wintsche, B., Glaser, K., Sträuber, H., Centler, F., Liebetrau, J., Harms, H., et al. (2016). Trace elements induce predominance among methanogenic activity in anaerobic digestion. *Front. Microbiol.* 7:2034. doi: 10.3389/fmicb.2016.02034

Wirth, R., Kovács, E., Maróti, G., Bagi, Z., Rákhely, G., and Kovács, K. L. (2012). Characterization of a biogas-producing microbial community by short-read next generation DNA sequencing. *Biotechnol. Biofuels* 5:41. doi: 10.1186/1754-6834-5-41

Wirth, R., Lakatos, G., Böjti, T., Maróti, G., Bagi, Z., Kis, M., et al. (2015). Metagenome changes in the mesophilic biogas-producing community during fermentation of the green alga Scenedesmus obliquus. *J. Biotechnol.* 215, 52–61. doi: 10.1016/j.jbiotec.2015.06.396

Wu, Y. W., Simmons, B. A., and Singer, S. W. (2016). MaxBin 2.0: an automated binning algorithm to recover genomes from multiple metagenomic datasets. *Bioinformatics* 32, 605–607. doi: 10.1093/bioinformatics/btv638

Ziganshin, A. M., Ziganshina, E. E., Kleinsteuber, S., and Nikolausz, M. (2016). Comparative analysis of methanogenic communities in different laboratory-scale anaerobic digesters. *Archaea* 2016:3401272. doi: 10.1155/2016/3401272

Conflict of Interest: The authors declare that the research was conducted in the absence of any commercial or financial relationships that could be construed as a potential conflict of interest.